

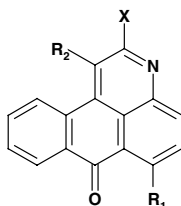
## Contents

### ARTICLES

#### Synthesis of 7-oxo-7*H*-naphtho[1,2,3-*de*]quinoline derivatives as potential anticancer agents active on multidrug resistant cell lines

pp 2880–2886

Maria Dzieduszycka, Maria M. Bontemps-Gracz, Barbara Stefańska, Sante Martelli, Agnieszka Piwkowska, Małgorzata Arciemiuk and Edward Borowski\*



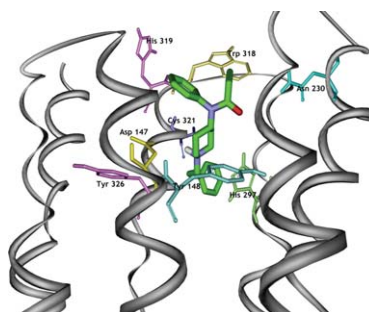
A series of 7-oxo-7*H*-naphtho[1,2,3-*de*]quinoline derivatives were synthesized and evaluated for their cytotoxic activity toward human leukemia sensitive and multidrug resistant cell lines.

#### Steric interactions and the activity of fentanyl analogs at the $\mu$ -opioid receptor

pp 2887–2895

Ljiljana Dosen-Micovic,\* Milovan Ivanovic and Vuk Micovic

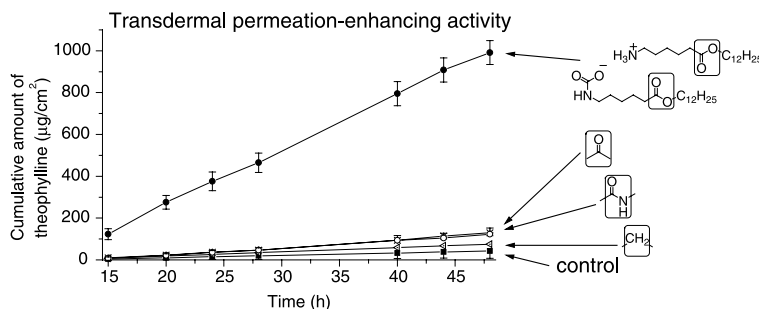
The interaction mechanism of a series of fentanyl analogs with  $\mu$ -opioid receptor was studied using flexible molecular docking simulations. Proposed orientations of fentanyl analogs in the binding pocket explain great variation in their enantiospecific potency and binding.



#### Synthesis and transdermal permeation-enhancing activity of ketone, amide, and alkane analogs of Transkarbam 12

pp 2896–2903

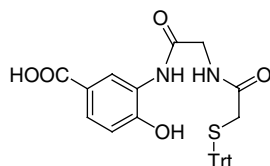
Tomáš Holas, Kateřina Vávrová,\* Jana Klimentová and Alexandr Hrabálek



### Synthesis, metal complexation and biological evaluation of a novel semi-rigid bifunctional chelating agent for $^{99m}\text{Tc}$ labelling

pp 2904–2909

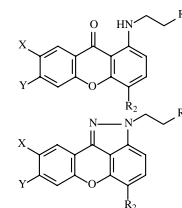
Julien Le Gal, Sandra Michaud, Marie Gressier, Yvon Coulais and Eric Benoist\*



In this paper, we report a convenient synthesis of a novel semi-rigid bifunctional chelating agent, their complexes with rhenium (V) and the in vivo behaviour in normal rats of the corresponding  $^{99m}\text{TcO}$ -complex.

### Design and synthesis of novel amino-substituted xanthenones and benzo[*b*]xanthenones: Evaluation of their antiproliferative activity and their ability to overcome multidrug resistance toward MES-SA/D $\times$ 5 cells

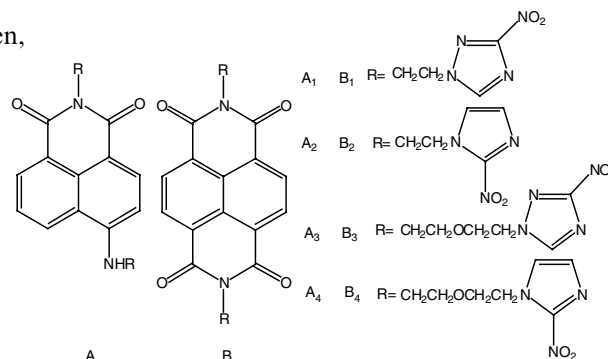
pp 2910–2934

Ioannis K. Kostakis, Nicole Pouli, Panagiotis Marakos,\*  
Alexios-Leandros Skaltsounis, Harris Pratsinis and Dimitris Kletsas

X= Y= H, C<sub>4</sub>H<sub>4</sub>, R<sub>1</sub>= N(CH<sub>3</sub>)<sub>2</sub>,  
N(C<sub>2</sub>H<sub>5</sub>)<sub>2</sub>, N(CH<sub>2</sub>)<sub>4</sub>, N(CH<sub>2</sub>)<sub>5</sub>,  
R<sub>2</sub>= H, NO<sub>2</sub>, NHC(=O)CH<sub>2</sub>R<sub>1</sub>

### Novel fluorescent markers for hypoxic cells of naphthalimides with two heterocyclic side chains for bioreductive binding

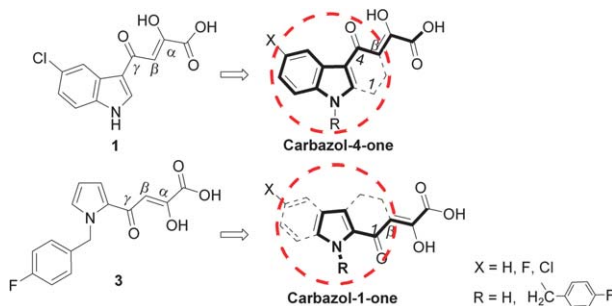
pp 2935–2941

Yan Liu, Yufang Xu,\* Xuhong Qian,\* Jianwen Liu, Liyun Shen,  
Junhui Li and Yuanxing Zhang

### Conformationally restrained carbazolone-containing $\alpha,\gamma$ -diketo acids as inhibitors of HIV integrase

pp 2942–2955

Xingnan Li and Robert Vince\*



### Dicationic pyridium porphyrins appending different peripheral substituents: Synthesis and studies for their interactions with DNA

pp 2956–2965

Song Wu, Zheng Li, Lige Ren, Bo Chen, Feng Liang, Xiang Zhou,\* Tao Jia and Xiaoping Cao

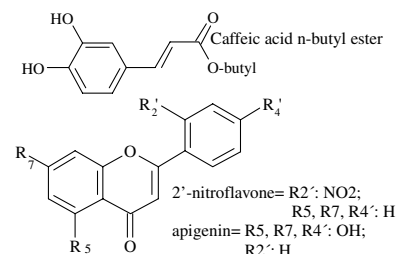
Twelve *trans*-dicationic pyridium porphyrins appending different peripheral substituents were synthesized and their abilities to bind and cleave DNA under irradiation have been investigated. Their binding modes to DNA were studied by UV–vis spectroscopy, circular dichroism. The apparent constants were measured by EB competitive fluorescence method and most of them were in the range of  $10^4$ – $10^5$  M<sup>-1</sup>. We found that both the position of positive charges and steric hindrance could greatly influence their binding affinities and modes to DNA, and then affect their photocleavage abilities to DNA.

### Antitumor activity of some natural flavonoids and synthetic derivatives on various human and murine cancer cell lines

pp 2966–2971

Mariano Cárdenas, Mariel Marder, Viviana C. Blank and Leonor P. Roguin\*

The *in vitro* activity of different natural flavonoids, cinnamic acid derivatives, and a series of synthetic flavones in established cancer cell lines was studied. Analysis of each group of compounds indicated that apigenin, caffeic acid *n*-butyl ester, and 2'-nitroflavone possess the most potent antiproliferative activities. In addition, a structure–activity relationship study was performed.

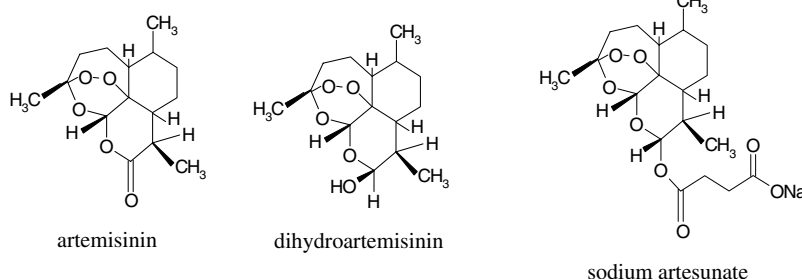


### The reaction of artemisinins with hemoglobin: A unified picture

pp 2972–2977

Luigi Messori,\* Chiara Gabbiani, Angela Casini, Matteo Siragusa, Franco Francesco Vincieri and Anna Rita Bilia

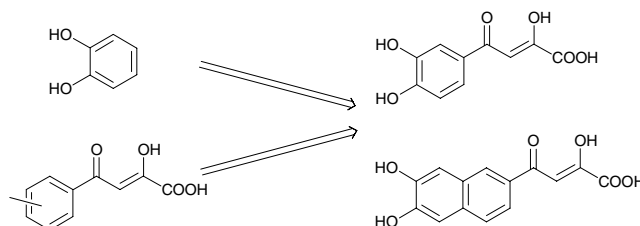
The reactions of artemisinin, sodium artesunate, and dihydroartemisinin with hemoglobin were investigated by visible absorption spectroscopy; a unified interpretation of the observed reactivity patterns is provided.



### Design, synthesis, and anti-integrase activity of catechol–DKA hybrids

pp 2978–2984

Cédric Maurin, Fabrice Bailly, Gladys Mbemba, Jean François Mouscadet and Philippe Cotelte\*

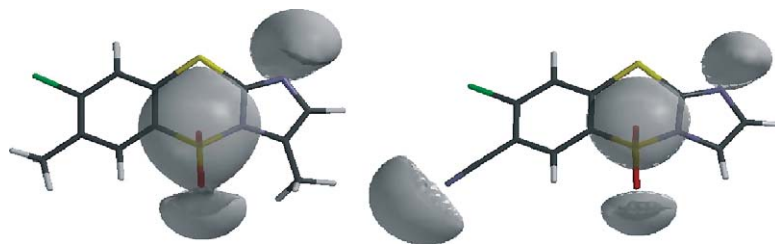


We designed and synthesized a new series of catechol–diketoacid hybrids as HIV-1 integrase inhibitors. The strand transfer/3'-processing selectivity was affected by the presence of the catechol moiety. These compounds presented micromolar anti-integrase activities with moderate antiviral properties.

**Synthesis, antitumor and anti-HIV activities of benzodithiazine-dioxides**

pp 2985–2993

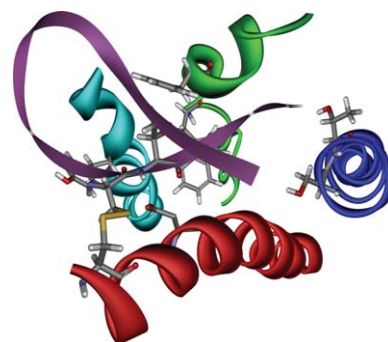
Zdzisław Brzozowski, Franciszek Sączewski\* and Nouri Neamati

**Interaction of arylpiperazine ligands with the hydrophobic part of the 5-HT<sub>1A</sub> receptor binding site**

pp 2994–3001

Mario V. Zlatović,\* Vladimir V. Šukalović, Christoph Schneider and Goran M. Roglić

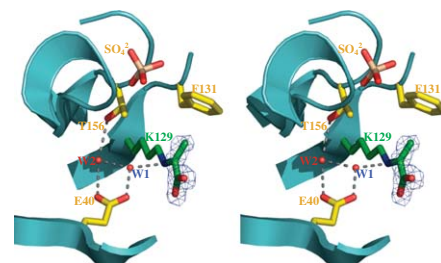
A flexible docking of a series of arylpiperazine derivatives with structurally different aryl part to the binding site of a model of human 5-HT<sub>1A</sub> receptor was exercised. The influence of structure and hydrophobic properties of aryl moiety on binding affinities was discussed and a model for ligand binding in the hydrophobic part of the binding site was proposed.

**Mechanism of the Class I KDPG aldolase**

pp 3002–3010

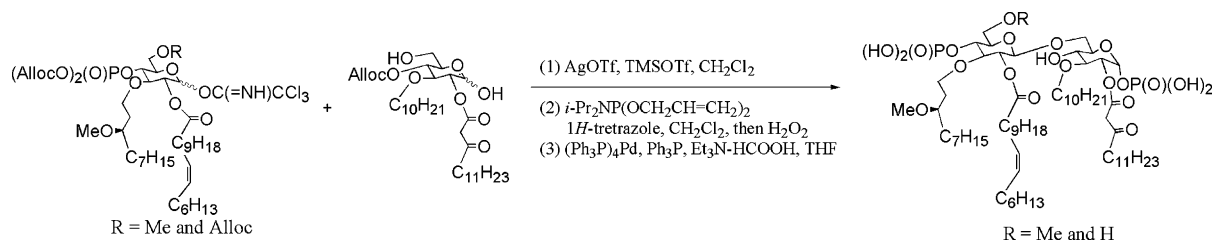
Stephen W.B. Fullerton, Jennifer S. Griffiths, Alexandra B. Merkel, Manoj Cheriyan, Nathan J. Wymer, Michael J. Hutchins, Carol A. Fierke,\* Eric J. Toone\* and James H. Naismith\*

A mechanism for catalysis by the Class I aldolase 2-keto-3-deoxy-6-phosphogluconate aldolase is reported based on crystallographic studies of native and mutant variants of both the *Thermotoga maritima* and *Escherichia coli* KDPG aldolase.

**Syntheses of glucose analogues of E5564 as a highly potent anti-sepsis drug candidate**

pp 3011–3016

Masao Shiozaki,\* Hiromi Doi, Daisuke Tanaka, Takaichi Shimozato and Shin-ichi Kurakata

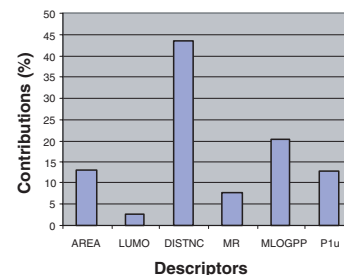


**QSAR modeling of mono- and bis-quaternary ammonium salts that act as antagonists at neuronal nicotinic acetylcholine receptors mediating dopamine release**

pp 3017–3037

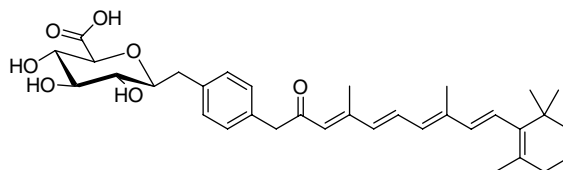
Fang Zheng, Ersin Bayram, Sangeetha P. Sumithran, Joshua T. Ayers, Chang-Guo Zhan, Jeffrey D. Schmitt, Linda P. Dwoskin and Peter A. Crooks\*

Back-propagation artificial neural networks were trained to model structure–activity relationships of mono- and bis-quaternary ammonium salts for the neural nicotinic acetylcholine receptor subtypes responsible for mediating nicotine-evoked dopamine release. A detailed analysis of the modeling results reveals relative contributions of the used descriptors to the trained ANN QSAR model, that is, ~44.0% from the length of the alkyl chain attached to a molecular head group, ~20.0% from Moriguchi octanol–water partition coefficient of the molecule, ~13.0% from molecular surface area, ~12.6% from the first component shape directional WHIM index/unweighted, ~7.8% from Ghose–Crippen molar refractivity, and 2.6% from the lowest unoccupied molecular orbital energy.

**Synthesis and preliminary chemotherapeutic evaluation of the fully C-linked glucuronide of N-(4-hydroxyphenyl)retinamide**

pp 3038–3048

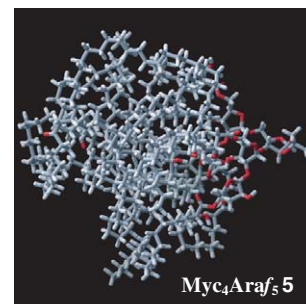
Joel R. Walker, Galal Alshafie, Nirca Nieves, Jamie Ahrens, Margaret Clagett-Dame, Hussein Abou-Issa and Robert W. Curley, Jr.\*

**Synthesis and TNF- $\alpha$  inducing activities of mycoloyl-arabinan motif of mycobacterial cell wall components**

pp 3049–3061

Akihiro Ishiwata, Hiroko Akao, Yukishige Ito,\* Makoto Sunagawa, Naoto Kusunose and Yasuo Kashiwazaki

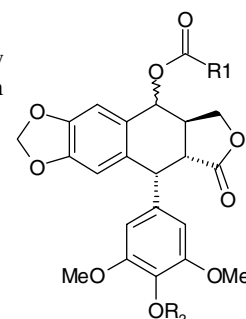
The aim of this study was to synthesize a series of mono- (1), di- (2, 3, 4) and tetramycolated (5) arabinans, which constitute the terminal region of BCG-CWS. In addition, their activities to induce TNF- $\alpha$  were evaluated.

**Synthesis and biological evaluation of new spin-labeled derivatives of podophyllotoxin**

pp 3062–3068

Yan Jin, Shi-Wu Chen and Xuan Tian\*

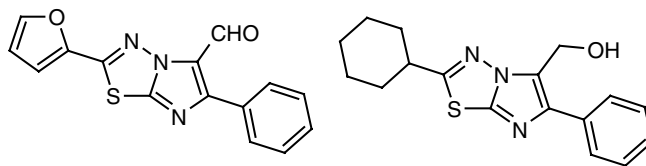
Target compounds with 4 $\beta$ -stable nitroxides and (or) 4'-hydroxyl ester showed generally superior cytotoxicities than VP-16, and their antioxidative activities were in accord with antitumor activities.

4'Á, R<sub>2</sub>=CH<sub>3</sub>; 4'Á, R<sub>2</sub>=H, COR<sub>1</sub>

**Synthesis and evaluation of antitubercular activity of imidazo[2,1-*b*][1,3,4]thiadiazole derivatives**

pp 3069–3080

Gundurao Kolavi, Vinayak Hegde, Imtiyaz ahmed Khazi\* and Pramod Gadad



The synthesis of the powerful antitubercular agents with 100% inhibitory activity (MIC > 6.25 µg/ml), antibacterial and antifungal agents is reported.

**Site-specific recombination of asymmetric *lox* sites mediated by a heterotetrameric Cre recombinase complex**

pp 3081–3089

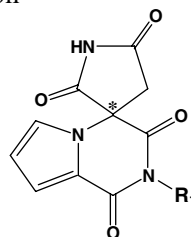
Talia Saraf-Levy, Stephen W. Santoro, Hanne Volpin, Tzvika Kushnirsky, Yoram Eyal, Peter G. Schultz, David Gidoni and Nir Carmi\*

Previous reports have demonstrated that new Cre recombinase specificities can be developed for symmetrically designed *lox* mutants through directed evolution. The development of Cre variants that allow the recombination of true asymmetric *lox* mutant sites has not yet been addressed, however. In the present study, we demonstrate that a mixture of two different site-specific Cre recombinase molecules (wt Cre and a mutant Cre) catalyzes efficient recombination between two asymmetric *lox* sites in vitro, presumably via formation of a functionally active heterotetrameric complex. The results may broaden the application of site-specific recombination in basic and applied research, including the custom-design of recombinases for natural, asymmetric, *lox*-related target sequences present in the genome. Future applications may potentially include genomic manipulations, for example, site-specific integrations, deletions or substitutions within precise regions of the genomes of mammals and other organisms.

**Quantitative structure–activity relationship of spirosuccinimide type aldose reductase inhibitors diminishing sorbitol accumulation in vivo**

pp 3090–3097

Kwangseok Ko, Hoshik Won\* and Youngdo Won\*

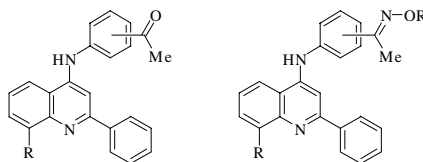


Quantitative structure–activity relationship of spirosuccinimide type aldose reductase inhibitors and the in vivo inhibitory activity of sorbitol accumulation is investigated with racemate physicochemical descriptors.

**Synthesis and antiproliferative evaluation of certain 4-anilino-8-methoxy-2-phenylquinoline and 4-anilino-8-hydroxy-2-phenylquinoline derivatives**

pp 3098–3105

Yeh-Long Chen, Chao-Jhieh Huang, Zun-Yuan Huang, Chih-Hua Tseng, Feng-Shuo Chang, Sheng-Huei Yang, Shinne-Ren Lin and Cherng-Chyi Tzeng\*



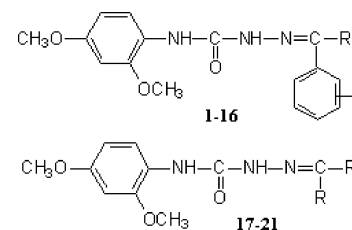
A number of 4-anilino-2-phenylquinoline derivatives were synthesized and evaluated for antiproliferative activity.

## 2,4-Dimethoxyphenylsemicarbazones with anticonvulsant activity against three animal models of seizures: Synthesis and pharmacological evaluation

pp 3106–3112

Rathinasabapathy Thirumurugan, Dharmarajan Sriram, Amrita Saxena, James Stables and Perumal Yogeeswari\*

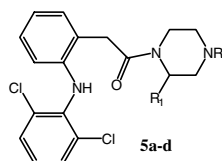
Various 2,4-dimethoxyphenylsemicarbazones were synthesized and the anticonvulsant evaluation was carried out using maximal electroshock seizure, subcutaneous pentylenetetrazole, and subcutaneous strychnine-induced seizure screens. Nine compounds exhibited protection in all the three seizure models, and *N*<sup>1</sup>-(2,4-dimethoxyphenyl)-*N*<sup>4</sup>-(propan-2-one)semicarbazone (**17**) emerged as the most active compound with no neurotoxicity.



## Synthesis, in vitro and in vivo antimycobacterial activities of diclofenac acid hydrazones and amides

pp 3113–3118

Dharmarajan Sriram,\* Perumal Yogeeswari and Ruth Vandana Devakaram

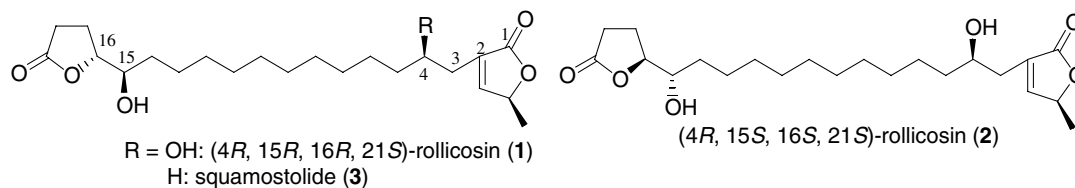


Various diclofenac acid hydrazones and amides were synthesized and evaluated for in vitro and in vivo antimycobacterial activities against *Mycobacterium tuberculosis*. Among the synthesized compounds, 1-cyclopropyl-6-fluoro-8-methoxy-7-[[*N*<sup>4</sup>-(2-(2-(2,6-dichlorophenylamino)phenyl)acetyl)-3-methyl]-*N*<sup>1</sup>-piperazinyl]-4-oxo-1,4-dihydro-3-quinoline carboxylic acid (**5d**) was found to be the most active compound in vitro with MIC of 0.0383  $\mu$ M and was more potent than the first line antitubercular drug isoniazid (MIC: 0.1822  $\mu$ M).

## Synthesis of (4*R*,15*R*,16*R*,21*S*)- and (4*R*,15*S*,16*S*,21*S*)-rollicosin, squamostolide, and their inhibitory action with bovine heart mitochondrial complex I

pp 3119–3130

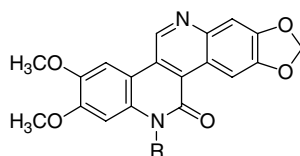
Hidefumi Makabe,\* Yuka Kimura, Masaharu Higuchi, Hiroyuki Konno, Masatoshi Murai and Hideto Miyoshi



## 6-Substituted 6*H*-dibenzo[*c,h*][2,6]naphthyridin-5-ones: Reversed lactam analogues of ARC-111 with potent topoisomerase I-targeting activity and cytotoxicity

pp 3131–3143

Shejin Zhu, Alexander L. Ruchelman, Nai Zhou, Angela Liu, Leroy F. Liu and Edmond J. LaVoie\*



where R is CH<sub>2</sub>CH<sub>2</sub>N(CH<sub>3</sub>)<sub>2</sub>; CH<sub>2</sub>CH(CH<sub>3</sub>)N(CH<sub>3</sub>)<sub>2</sub>; CH<sub>2</sub>CH<sub>2</sub>N(CH<sub>2</sub>CH<sub>3</sub>)<sub>2</sub>; CH<sub>2</sub>CH<sub>2</sub>N(–CH<sub>2</sub>CH<sub>2</sub>CH<sub>2</sub>CH<sub>2</sub>–); CH<sub>2</sub>CH<sub>2</sub>N(–CH<sub>2</sub>(CH<sub>2</sub>)<sub>3</sub>CH<sub>2</sub>–); CH<sub>2</sub>CH<sub>2</sub>N(–CH<sub>2</sub>CH<sub>2</sub>OCH<sub>2</sub>CH<sub>2</sub>–); CH<sub>2</sub>CH<sub>2</sub>CH<sub>2</sub>N(CH<sub>3</sub>)<sub>2</sub>; CH<sub>2</sub>CH<sub>2</sub>(–CHN(CH<sub>3</sub>)CH<sub>2</sub>CH<sub>2</sub>CH<sub>2</sub>–); CH<sub>2</sub>CH<sub>2</sub>N(Bn)<sub>2</sub>; CH<sub>2</sub>CH<sub>2</sub>N(CH<sub>3</sub>)Bn; CH<sub>2</sub>CH<sub>2</sub>NH<sub>2</sub>; CH<sub>2</sub>CH<sub>2</sub>NHCH<sub>3</sub>.

**3D QSAR on a library of heterocyclic diamidine derivatives with antiparasitic activity**

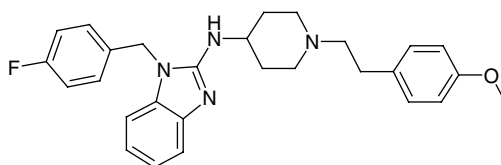
pp 3144–3152

Prashanth Athri, Tanja Wenzler, Patricia Ruiz, Reto Brun, David W. Boykin, Richard Tidwell and W. David Wilson\*

**Prediction of hERG potassium channel affinity by the CODESSA approach**

pp 3153–3159

Alessio Coi, Ilaria Massarelli, Laura Murgia, Marilena Saraceno, Vincenzo Calderone and Anna Maria Bianucci\*

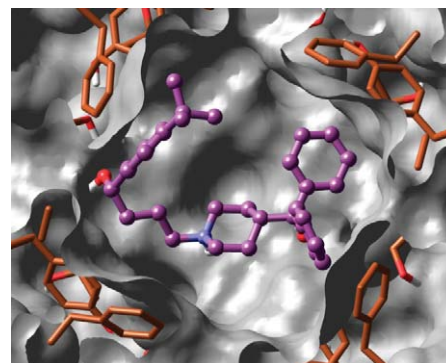


Astemizole, withdrawn from the market due to QT prolongation concerns. CODESSA program is exploited to propose a method for the prediction of torsadogenic cardiotoxicity of drugs due to hERG channel blockade.

**New insights about HERG blockade obtained from protein modeling, potential energy mapping, and docking studies**

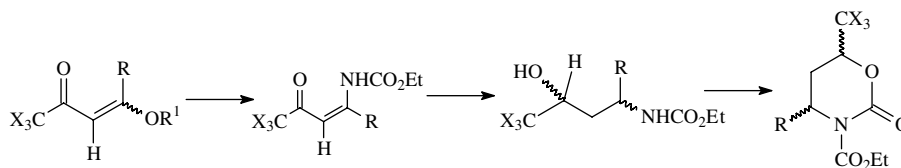
pp 3160–3173

Ramy Farid,\* Tyler Day, Richard A. Friesner and Robert A. Pearlstein

**Synthesis and antimicrobial activity of new (4,4,4-trihalo-3-oxo-but-1-enyl)-carbamic acid ethyl esters, (4,4,4-trihalo-3-hydroxy-butyl)-carbamic acid ethyl esters, and 2-oxo-6-trihalomethyl-[1,3]oxazinane-3-carboxylic acid ethyl esters**

pp 3174–3184

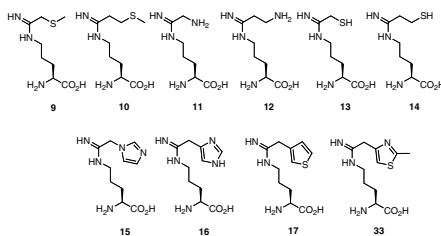
Nilo Zanatta,\* Deise M. Borchhardt, Sydney H. Alves, Helena S. Coelho, Adriana M. C. Squizani, Tiago M. Marchi, Helio G. Bonacorso and Marcos A. P. Martins



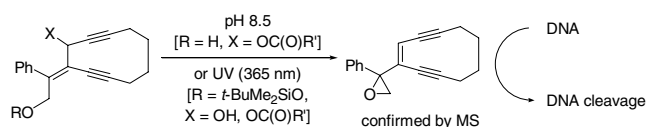
X = F, Cl; R = H, Me, Ph, 4-Me-Ph



**Design, synthesis, and biological testing of potential heme-coordinating nitric oxide synthase inhibitors** pp 3185–3198  
Elizabeth A. Litzinger, Pavel Martásek, Linda J. Roman and Richard B. Silverman\*

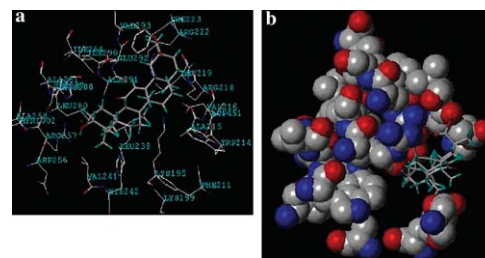


**Synthesis and DNA cleavage reaction characteristics of enediyne prodrugs activated via an allylic rearrangement by base or UV irradiation** pp 3199–3209  
Yukihiro Tachi, Wei-Min Dai,\* Kazuhito Tanabe and Sei-ichi Nishimoto\*

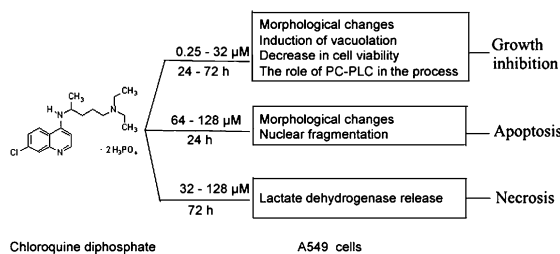


**Binding analysis of glycyrrhetinic acid to human serum albumin: Fluorescence spectroscopy, FTIR, and molecular modeling** pp 3210–3217  
Jianghong Tang, Feng Luan and Xingguo Chen\*

The interaction model between glycyrrhetinic acid (GEA) and HSA. (a) Only residues around 6.5 Å of GEA are displayed. The residues of HSA are represented using lines and the GEA structure is represented using a stick model. (b) GEA–HSA spacefill conformation. Protein atoms are shown in CPK representation and the GEA structure is represented using a stick model. The model shown GEA can bind to subdomain IIA of HSA, namely, site I. This result indicated that hydrophobic interaction played an important role.



**Chloroquine inhibits cell growth and induces cell death in A549 lung cancer cells** pp 3218–3222  
Chuandong Fan, Weiwei Wang, Baoxiang Zhao,\* Shangli Zhang and Junying Miao\*

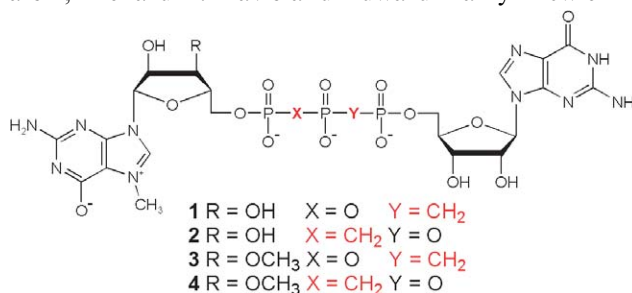


Chloroquine diphosphate (CQ) could inhibit cell growth, elicit cell apoptosis, and induce necrosis in A549 cells at different concentrations. Moreover, the results suggested the involvement of PC-PLC in cell growth inhibition by CQ at lower concentrations.

### Enzymatically stable 5' mRNA cap analogs: Synthesis and binding studies with human DcpS decapping enzyme

pp 3223–3230

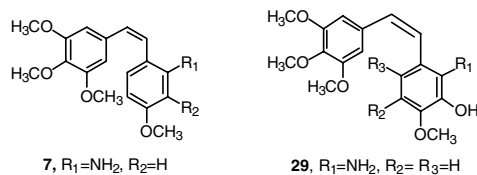
Marcin Kalek, Jacek Jemielity, Zbigniew M. Darzynkiewicz, Elzbieta Bojarska, Janusz Stepinski, Ryszard Stolarski, Richard E. Davis and Edward Darzynkiewicz\*



### Design, synthesis, and biological evaluation of combretastatin nitrogen-containing derivatives as inhibitors of tubulin assembly and vascular disrupting agents

pp 3231–3244

Keith A. Monk, Rogelio Siles, Mallinath B. Hadimani, Benon E. Mugabe, J. Freeland Ackley, Scott W. Studerus, Klaus Edvardsen, Mary Lynn Trawick, Charles M. Garner, Monte R. Rhodes, George R. Pettit and Kevin G. Pinney\*



## OTHER CONTENTS

### Erratum

p 3245

### Summary of instructions to authors

p I

\*Corresponding author

Supplementary data available via ScienceDirect

**COVER**

2006: The cover figure shows a synthetic multifunctional pore that is composed of rigid-rod staves (para-octiphenyls, tan) and beta-sheet hoops (arrows) and can be activated with external ligands (fullerenes, golden spheres) and closed with internal blockers (alpha-helix, red ribbon) [Gorteau, V.; Bollot, G.; Mareda, J.; Pasini, D.; Tran, D.-H.; Lazar, A. N.; Coleman, A. W.; Sakai, N.; Matile, S. *Bioorg. Med. Chem.* **2005**, *13*, 5171–5180].



Full text of this journal is available, on-line from **ScienceDirect**. Visit [www.sciencedirect.com](http://www.sciencedirect.com) for more information.



This journal is part of **ContentsDirect**, the *free* alerting service which sends tables of contents by e-mail for Elsevier books and journals. You can register for **ContentsDirect** online at: <http://contentsdirect.elsevier.com>

---

Indexed/Abstracted in: Beilstein, Biochemistry & Biophysics Citation Index, CANCERLIT, Chemical Abstracts, Chemistry Citation Index, Current Awareness in Biological Sciences/BIOBASE, Current Contents: Life Sciences, EMBASE/Excerpta Medica, MEDLINE, PASCAL, Research Alert, Science Citation Index, SciSearch, TOXFILE



ELSEVIER

ISSN 0968-0896